Alternate synthetic strategy for the preparation of CdS nanoparticles and its exploitation for water splitting

M. Sathish, B. Viswanathan, R.P. Viswanath*

Department of Chemistry, Indian Institute of Technology Madras, Chennai-600 036, India

Available online 12 September 2005

Abstract

Cadmium sulphide nanoparticles (6–12 nm) are prepared by a precipitation process using different zeolite matrices as templates. The nanoparticles were characterized by UV-Vis, XRD, SEM, TEM and sorptometric techniques. XRD study shows the presence of hexagonal and cubic phases for the nanoparticles whereas in case of the bulk samples only the hexagonal phase is observed. These nanomaterials have been used as catalysts for the photocatalytic decomposition of water. The nanoparticles show a higher hydrogen evolution rate compared to the bulk samples which correlates well with the particle size and surface area. Noble metal (Pt, Pd, Rh, Ru)-loaded samples were subsequently prepared and tested for hydrogen evolution reaction. The presence of Pt metal is found to enhance the hydrogen production rate whereas the hydrogen production rate is retarded in the presence of Ru metal. This has been explained on the basis of metal hydrogen bond, redox potential and work function of the noble metal.

© 2005 International Association for Hydrogen Energy. Published by Elsevier Ltd. All rights reserved.

Keywords: Photocatalyst; Hydrogen production; CdS nanoparticles; Water splitting; Zeolite template

1. Introduction

Production of hydrogen from an inexhaustible source, water, by a cheaper route has been under extensive investigations in recent years [1,2]. Among different processes used for hydrogen production, photocatalysis is a method which has to be improved in terms of viability where sunlight can be utilized as a sustainable energy source for hydrogen production. Selection of a suitable photocatalyst is an important criterion to establish the process as workable for the maximum quantity of hydrogen production. Essentially, the photocatalyst should have appropriate conduction and valence band edge positions in order to reduce and oxidize the H^+ and OH^- ions, respectively. For better hydrogen

evolution activity, the bottom of the conduction band should have more negative potential than the H^+/H_2 redox potential. The values of the top edge of the valence band should be more positive with the oxidation potential of water. In addition to these criteria, the photocatalyst should absorb light especially in the visible region and should have good photo-stability under the irradiation conditions.

Several types of semiconducting materials such as TiO_2, CdS, ZnO and Fe_2O_3 have been investigated for hydrogen production [3–5]. Among them CdS shows light absorption in the visible region and has suitable conduction band potential to reduce the H^+ ion effectively. However, the utility of CdS as a photocatalyst has been limited due to its anodic decomposition, the so-called photocorrosion. A number of attempts have been made to overcome this disadvantage by using suitable sacrificial agents. In general, an Na_2S and Na_2SO_3 mixture has been widely used as a sacrificial agent [6]. Coupling of CdS with other semiconductors like TiO_2 and ZnS has also been studied [7]. It has been observed

* Corresponding author. Tel.: +91 44 22574216;
fax: +91 44 22574202.

E-mail address: rpv@iitm.ac.in (R.P. Viswanath).

that, the photocatalytic activity for hydrogen production increases considerably in the coupled semiconductors because of the interparticle electron transfer process [8]. In the coupled semiconductor photogenerated electron is transferred with relative ease, from one semiconductor to the other, due to the favourable position of the conduction bands of the semiconductor couple and this results in efficient electron transfer for H^+ ion reduction. Recently, $LaMnO_3/CdS$ [9] and CdS/ETS-4 (Titanosilicate zeolite) [10] composites have been studied as efficient catalysts for photocatalytic hydrogen production. It has been shown that the supported CdS shows a higher activity in the presence of a sacrificial agent without undergoing any photocorrosion. The surface characteristics of the support such as the acid–base properties can also play an important role in the photocatalytic activity of CdS. In case of the CdS/MgO photocatalyst, it has been observed that the activity for hydrogen reduction is enhanced with increasing basicity of the support [11,12]. Furthermore, it is known that semiconductor nanoparticles show a higher photocatalytic activity compared to the bulk materials [13,14] due to changes in the surface area, band gap, morphology and generation of surface defects. Various methods have been adopted in the literature for the synthesis of CdS nanoparticles [15–18] and CdS particles embedded in the cages, egg membrane and zeolite [19–21]. The photocatalytic experiments carried out using CdS-embedded systems show better activity than the bulk CdS although the nonactive host material can reduce the amount of light absorption. In order to overcome this problem, in this study CdS nanoparticles in a zeolite matrix have been prepared, which are subsequently retrieved by treatment with HF solution. The CdS nanoparticles prepared by this method were used to carry out photocatalytic hydrogen production. The photocatalytic activity of these materials has been found to correlate well with the particle size. The effect of noble metal loading on CdS for the photocatalytic hydrogen evolution has also been studied.

2. Experimental

2.1. Preparation of CdS catalysts

CdS nanoparticles were prepared by precipitation in the zeolite matrix. Three different zeolites (H-Y, HZSM-5 and H-β) with different pore sizes were used for this purpose. In a typical preparation procedure, 1 g of a sodium form of zeolites was taken in a round-bottom flask and 100 ml of 1 M $CdNO_3$ solution was added to it. The mixture was stirred for 24 h at room temperature. The zeolite was filtered and washed with distilled water until the filtrate was free from Cd^{2+} ions. The sample was dried and stirred with 100 ml of 1 M Na_2S solution for 12 h, leading to the precipitation of the cadmium ions present inside the zeolite matrix. The precipitated CdS particles were washed with distilled water until the filtrate was free from the S^{2-} ions. Finally,

the zeolite matrix was removed by treatment with 48% HF solution. The undissolved CdS particles were washed with hot water until the pH of the filtrate became neutral. For the sake of comparison, bulk CdS particles were prepared by a conventional precipitation method. In this method, an equimolar amount of Na_2S solution was added dropwise to a stirred solution of 1 M $Cd(NO_3)_2$ resulting in the formation of CdS precipitates. The CdS precipitate was washed repeatedly with distilled water until free from S^{2-} ions, dried in an air-oven and then calcined at 400 °C for 4 h in air. The CdS particles prepared from H-Y, HZSM-5 and H-β are described as CdS-Y, CdS-Z and CdS-B, respectively, in subsequent discussions.

2.2. Preparation of metal-loaded CdS catalysts

Pt, Pd, Ru and Rh metal-loaded CdS was also prepared by impregnation of corresponding metal chlorides with CdS particles followed by reduction in H_2 atmosphere at 723 K. Generally, 1 wt% of noble metal was loaded on to the CdS particles prepared from various zeolite matrixes.

2.3. Characterization

Powder X-ray diffraction patterns of the CdS samples were recorded using a SHIMADZU XD- D1 diffractometer using Ni-filtered Cu Kα radiation ($\lambda = 1.5418$ Å). UV–Visible absorption spectra were recorded using a Cary 5E UV–Vis–NIR spectrophotometer in the spectral range of 200–800 nm. Absorption spectra for catalyst samples were recorded as nujol paste. The specific surface area, pore size and pore volume of the samples were measured using a Sorptomatic 1990 instrument at 77 K. Prior to the sorptometric experiment, the samples were degassed at 423 K for 12 h. The surface morphology of the CdS particles was obtained using a JEOL-JSM-5610LV scanning electron microscope (SEM). The transmission electron micrographs (TEM) were recorded with a JEOL-JEM 100SX microscope, working at a 100 kV accelerating voltage. Samples for TEM were prepared by dispersing the powdered sample in acetone by sonication and then drip drying on a copper grid (400 mesh) coated with carbon film.

2.4. Photocatalytic activity

Photocatalytic hydrogen evolution experiments were performed on these materials using a quartz reactor with options for water circulation at the outer wall of the reactor and specific outlet for gas collection. For a typical photocatalytic experiment, 0.1 g of catalyst was added to a 50 ml of aqueous solution containing 0.35 M Na_2SO_3 and 0.24 M Na_2S and placed inside the reactor. Before illumination by a UV source, the solution was de-aerated with nitrogen gas for 30 min to remove the dissolved oxygen. Then the mixture was irradiated with a 400 W Hg lamp (ORIEL

Corporation, USA). The evolved gas was collected over brine water using an inverted gas burette.

2.5. Product gas analysis

The gas products have been analysed using a chromatograph (Nucon-Model 5765) with molecular sieve 5A as a column and thermal conductivity detector (TCD). For the detection of hydrogen, nitrogen was used as the carrier gas and for that of oxygen/moisture, the carrier gas was hydrogen.

3. Results and discussion

3.1. UV–Visible spectra

UV–Visible absorption spectra for CdS nanoparticles prepared from different zeolite matrices are shown in Fig. 1. Comparing the absorption edge of bulk CdS with that of CdS-Y, CdS-Z and CdS-B samples prepared from different zeolites, it is seen that a blue shift in the onset of absorption is observed in these samples. This phenomenon of blue shift of absorption edge has been ascribed to a decrease in particle size. It is well known that in case of semiconductors the band gap between the valence and conduction band increases as the size of the particle decreases in the nanosize range. This results in a shift in the absorption edge to a lower wavelength region. The magnitude of the shift depends on the particle size of the semiconductor. In the present study, the CdS-Z samples prepared from the ZSM-5 zeolite matrix showed a blue shift of approximately 65 nm compared to the bulk particles. The smaller pore size and pore volume of the ZSM-5 compared to the other two zeolites are responsible for the formation of CdS with a small size. From the onset of the adsorption edge, the band gap of the CdS particles was calculated using the method of Tandon and Gupta [22]. In Table 1, the band gap is found to increase in the order CdS-Z > CdS-Y > CdS-B > CdS.

3.2. X-ray diffraction study

X-ray diffraction patterns of the prepared CdS nanoparticles using zeolite templates and HF-treated CdS bulk sample are presented in Fig. 2. The bulk CdS sample was treated with 48% HF solution for 12 h prior to the XRD study to observe any possible change in phase or crystallinity. The bulk CdS sample showed major X-ray reflections with *d* values of 3.56, 3.35, 3.15 and 2.06 corresponding to the hexagonal phase of cadmium sulphide (JCPDS No 06 -0314). In case of the CdS-Y, CdS-Z and CdS-B samples, in addition to the above-mentioned peaks a new peak was observed at a *d* value of 2.9 (indicated by an arrow). This peak corresponds to the cubic phase of the CdS particles (JCPDS No.10-0454). Peak broadening was also observed in case of the CdS nanoparticles prepared from zeolites compared
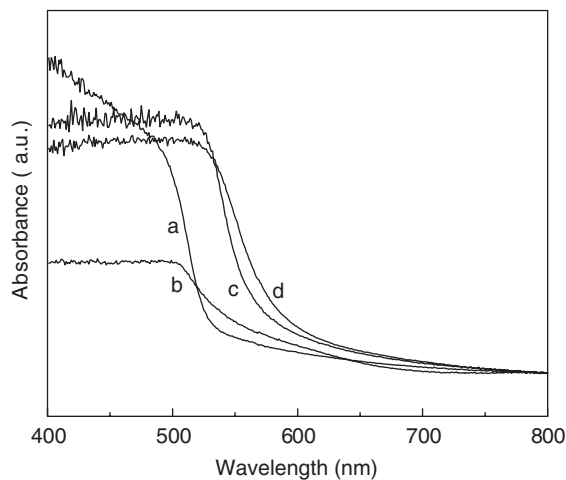
Fig. 1. UV–Visible absorbance spectra of (a) CdS-Z, (b) CdS-Y, (c) CdS-B and (d) bulk CdS.

Table 1
Band gap, particle size, specific surface area and pore volume of CdS samples prepared from zeolite and bulk CdS sample

Samples	Band gap (eV)	Particle size (nm)	Specific surface area ($m^2\,g^{-1}$)	Pore volume ($cm^3\,g^{-1}$)
CdS-Z	2.36	6	46	0.236
CdS-Y	2.25	8.8	36	0.123
CdS-B	2.21	11.6	26	0.073
CdS	2.13	23	14	0.042
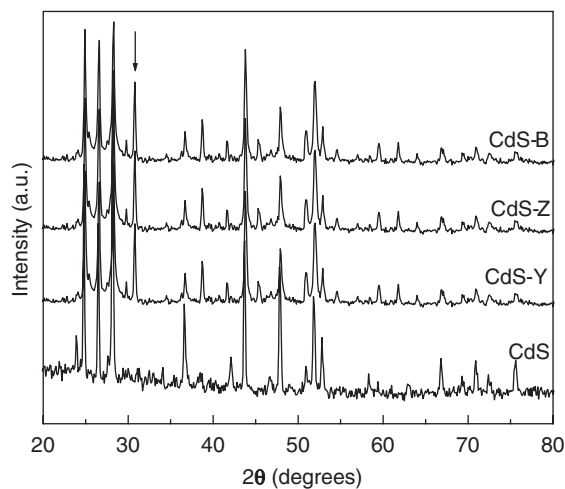
Fig. 2. X-ray diffraction patterns of bulk CdS and CdS nanoparticles.

to that of the bulk samples. The HF-treated CdS bulk sample showed XRD patterns identical to those of bulk CdS particles indicating that there was no significant change in
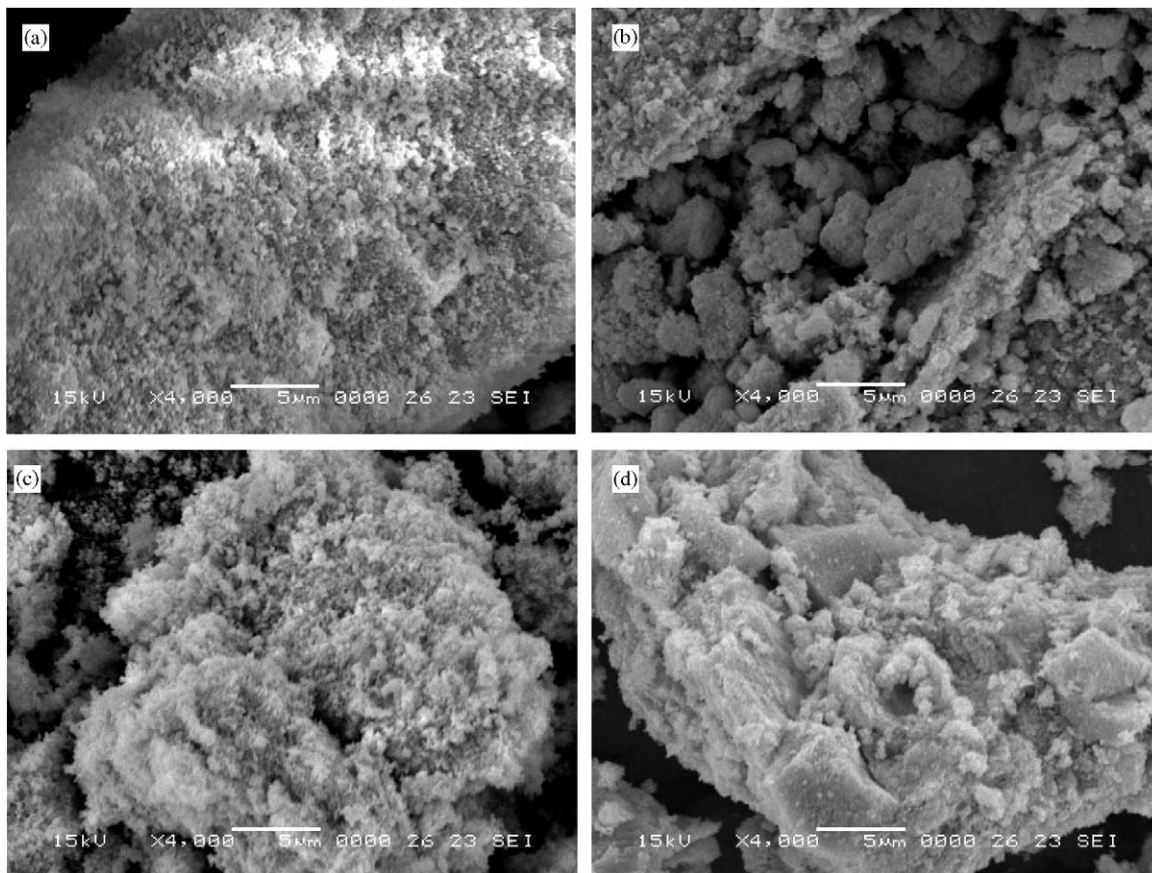
Fig. 3. SEM photographs of (a) CdS-Z, (b) CdS-Y, (c) CdS-B and (d) bulk CdS.

the crystal structure and phase as a result of the acid treatment. The XRD study clearly demonstrates that nanosize CdS particles with altered phases can be prepared by using the zeolite matrix as a template for synthesis.

The XRD patterns for the samples after treatment in hydrogen atmosphere at 723 K do not indicate any phase or morphological change.

3.3. Surface area and electron microscopic analysis

The specific surface area and pore volume of the CdS samples prepared from different sources are presented in Table 1. As can be seen from the table, the surface area of the CdS depends on the zeolite matrix from which it has been prepared. The highest surface area and pore volume were observed for the CdS-Z particles prepared from ZSM-5 zeolite. ZSM-5 is a medium pore size zeolite with a pore opening in the range of 5–6 Å. During the preparation process, CdS particles are homogeneously precipitated inside the pores of the Zeolites. Upon removal of the zeolite matrix uniform pores are created in the CdS particles. These pores contribute to a higher pore volume and surface area

of the CdS-Z sample. The same argument can be extended to the CdS-Y and CdS-B samples prepared from the H-Y and H-β zeolites, respectively.

The surface morphology of CdS nanoparticles has been studied by scanning electron microscopy. The SEM pictures of the CdS samples are presented in Fig. 3. The growth of fine particles of CdS in a regular pattern is observed on the surface of the CdS-Y, CdS-Z and CdS-B samples in Figs. 3a–c. The surface is also relatively rough for the CdS particles prepared from the zeolite matrices. In case of the bulk sample in Fig. 3d the surface is smooth with a large outgrowth of CdS particles in an irregular manner. The transmission electron micrograph of the CdS sample from Y zeolite is shown in Fig. 4. Particles in nanosize range are clearly observed for the CdS-Y, CdS-Z and CdS-B samples. The exact particle sizes for the bulk and the prepared samples have been calculated from the micrographs and are presented in the Table 1. It is observed that the nature of the zeolite matrix plays a vital role in the particle size. The CdS-Y and CdS-Z samples prepared from zeolites showed a lower particle size compared to other two samples.
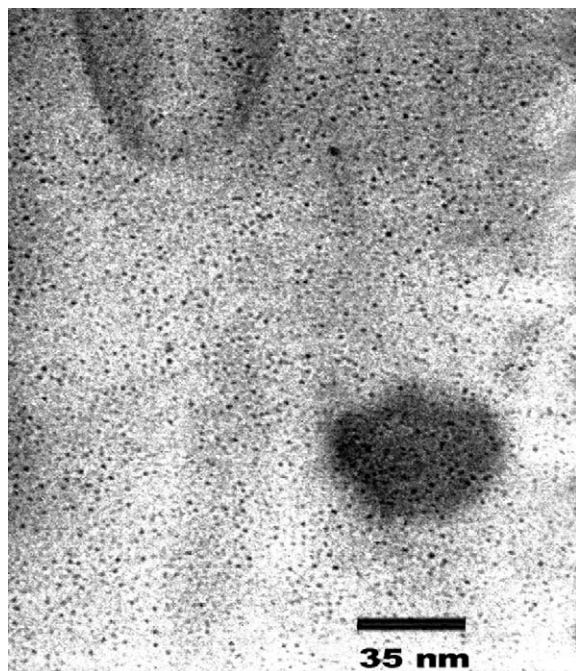
Fig. 4. TEM image of a CdS-Y sample.

Table 2
The rate of hydrogen production with different CdS samples

S.no.	Sample	Rate of hydrogen production (μmol h^{-1} 0.1 g^{-1})
1	CdS-Z	68
2	CdS-Y	102
3	CdS-β	67
4	CdS-B	45

3.4. Photocatalytic activity

Photocatalytic hydrogen evolution reaction has been carried out on these materials under ambient conditions. The amount of hydrogen evolved is presented in Table 2. From the results, it can be seen that the amount of hydrogen evolved is higher for the CdS nanoparticles in comparison with that of the bulk CdS samples. The CdS-Y prepared from an HY zeolite matrix showed a hydrogen evolution rate of 102 μmol h^{-1} when S^{2-}/SO_3^{2-} was used as a sacrificial agent. This value is quite significant in comparison with the other hydrogen evolution rate reported for pure CdS particles in the literature [8]. The higher hydrogen evolution rate in the present case can be ascribed to the lower particle size and high surface area of these materials. Fig. 5 shows that the amount of hydrogen evolved over different CdS samples for a time period of 6 h. For the sake of comparison, the CdS particles present inside the zeolite matrix were also tested
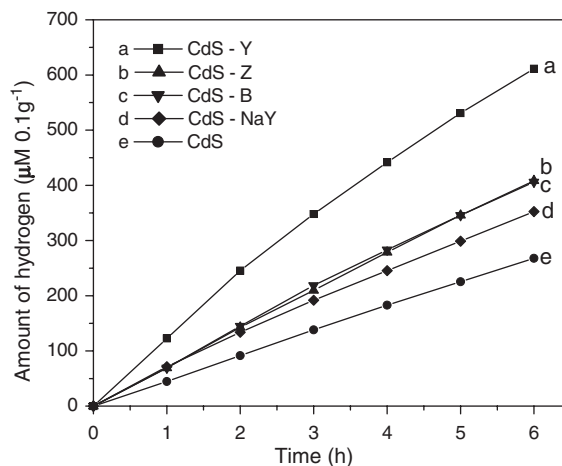
Fig. 5. Amount of hydrogen produced on (a) CdS-Y, (b) CdS-Z, (c) CdS-B, (d) Zeolite-Y containing CdS nanoparticles (CdS-H-Y) and (e) bulk CdS.

for hydrogen evolution under the same conditions. It was observed -that the nanoparticles show a higher activity compared to the CdS nanoparticles entrapped inside the zeolite matrix (without removing the zeolite matrix). This points to the fact that the inert zeolite matrix reduces the amount of light absorption by CdS nanoparticles, thereby reducing its activity. Also, during this 6 h period there was no appreciable decrease in the activity of these nanomaterials. After the catalytic experiments these catalysts were recovered and regenerated by washing in water and subsequently calcining at 673 K for 4 h. The regenerated catalysts showed similar activity as that of a fresh catalyst indicating that photocorrosion has been reduced substantially by using the sacrificial agent. In the present case, the Na_2S/Na_2SO_3 system is quite effective in preventing photo corrosion which has been well studied in the literature [6].

It is well known that the photocatalytic activity of CdS increases substantially in the presence of noble metal particles [23]. In order to study the effect of noble metals on the hydrogen evolution rate of these CdS samples, 1 wt% metal-loaded samples were prepared by impregnation method. The hydrogen evolution rates for various noble metal (Pt, Pd, Ru, Rh)-loaded CdS nanoparticles are shown in Fig. 6. Among the noble metals studied, Pt metal loaded on CdS prepared from ZSM-5 zeolite shows a higher hydrogen evolution rate. The rate of hydrogen production on a noble metal surface can be related to the metal hydrogen bond, redox potential and work function of the noble metal atom [24]. Hydrogen evolution increases linearly with increasing in redox potential of the noble metal. The more positive the redox potential of a metal, the faster the reduction of H$^+$ ion. Similarly, the hydrogen evolution; also depends on the metal–hydrogen bond strength. When the metal–hydrogen bond energy is less,
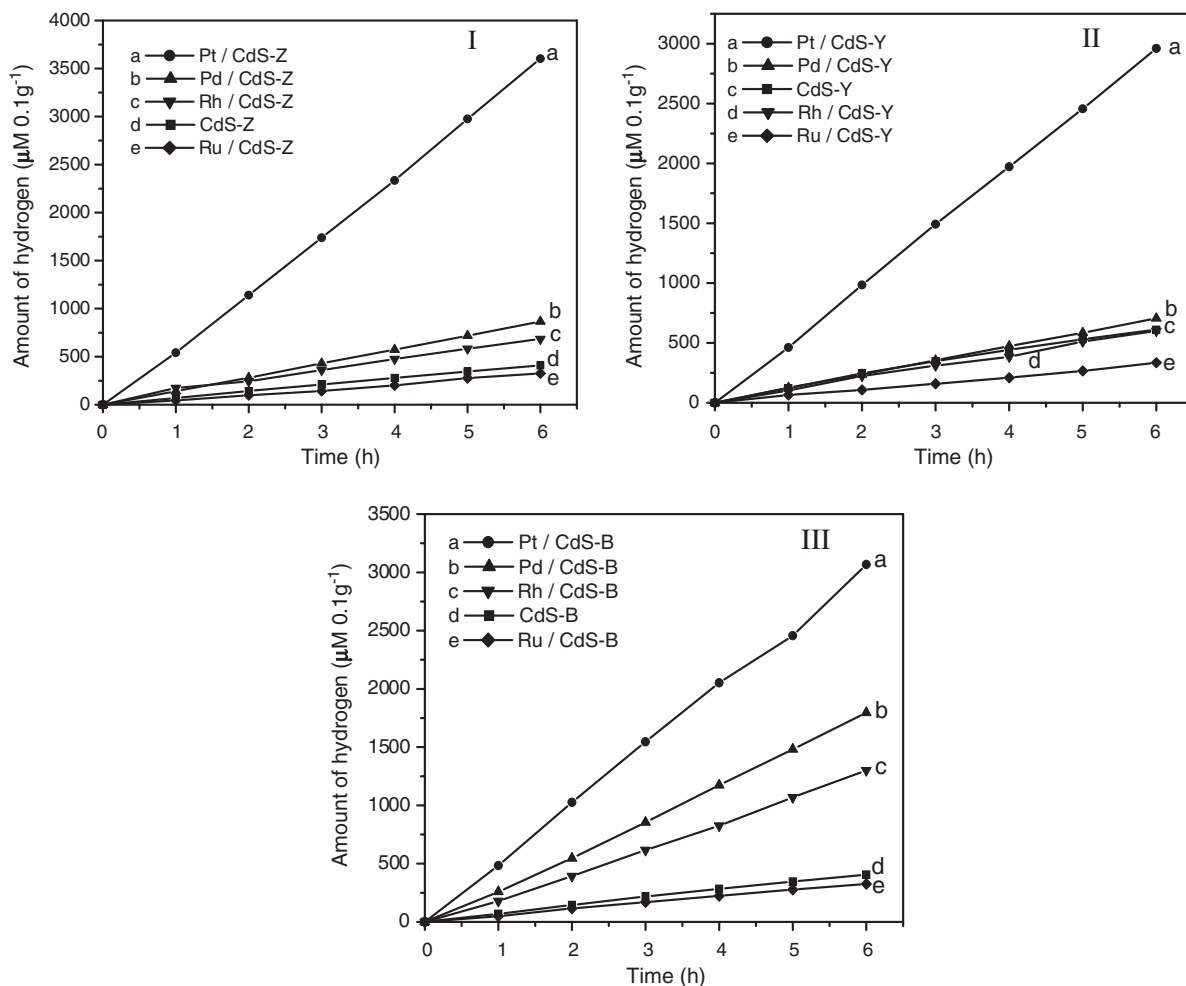
Fig. 6. Amount of hydrogen produced on (I) CdS-Z, (II) CdS-Y and (III) CdS-B.

the hydrogen evolution barrier is substantially reduced resulting in easy evolution of molecular hydrogen. The work function of the metal is another factor that influences the hydrogen evolution, if it is high, the reduction rate increases. These parameters are crucial for hydrogen evolution reactions and are tabulated in Table 3. From the table, it can be observed that there is a direct correlation between these factors and hydrogen evolution. Pt metal with a higher redox potential, work function and lower metal hydrogen bond strength is found to be favourable for hydrogen evolution activity, whereas in the case of the Ru-loaded CdS samples it has been observed that the hydrogen production activity is lower than the naked CdS. This is due to the strong Ruthenium–hydrogen bond which inhibits hydrogen evolution on the ruthenium surface. In this study, with 0.1 g of the Pt-loaded CdS nanoparticles the hydrogen evolution rate was found to be $600 \, \mu\text{mol} \, \text{h}^{-1}$ which is higher than the value reported so far in the literature [12].

Table 3
Redox potential, metal--hydrogen bond strength, work function and rate of hydrogen evolution for different noble metal-loaded CdS-Z samples

Metal	Redox potential (E^0)	Metal–hydrogen bond energy (K cal mol^{-1})	Work function (eV)	Hydrogen evolution rate[a] (μmol h^{-1} 0.1 g^{-1})
Pt	1.188	62.8	5.65	600
Pd	0.951	64.5	5.12	144
Rh	0.758	65.1	4.98	114
Ru	0.455	66.6	4.71	54

[a] 1 wt% metal loaded on a CdS-Z sample. The reaction data are presented after 6 h under a reaction condition.

3.5. Product analysis

It has been reported in the literature that in the photocatlysis using sulphide nano particles hydrogen gas is produced by the reduction of H^+ ions by the photo generated electrons from the conduction band of the semiconductor. The elemental sulphur is the other product. This reacts with excess sulphide ($S^=$) ions present to give a disulphide ($S_2^=$) ion. This further reacts with sulphite ions to regenerate sulphide ion along with thio sulphate ions. Thus in the presence of a mixture of sulphide and sulphite, hydrogen will be the only product. The evolved gas has been analysed and found to be hydrogen along with a trace quantity of moisture. The source of moisture may be due to the product gas, being generated from the reaction solution which is in aqueous medium, carrying water vapour along with it.

4. Conclusions

In this study, CdS nanoparticles prepared from zeolite matrices have been shown to be efficient photocatalysts for hydrogen production. The zeolite matrix acts as a templating agent preventing the growth of CdS particles during the precipitation process resulting in the formation of nanoparticles. The nanoparticles of CdS exhibit a blue shift in the absorption edge in the UV-DRS study due to particle size effect. Mixed cubic and hexagonal phases have been observed in the XRD study for the CdS nanoparticles prepared from the zeolites. The nanoparticles are of uniform size with a particle size distribution in the range of 6–12 nm. Photocatalytic activity studies on these materials clearly show that the nanoparticles exhibit higher activity compared to the bulk samples. Surface area, morphology and particle size of the CdS are important factors which affect their performance as catalysts for hydrogen evolution. The presence of noble metals such as Pt and Pd greatly enhances the photocatalytic activity of the synthesized CdS particles.

Acknowledgements

References

[1] So WW, Kim KJ, Moon SJ. Photo-production of hydrogen over the CdS-TiO₂ nano-composite particulate films treated with TiCl₄. Int J Hydrogen Energy 2003;29(3):229–34.

[2] Koca A, Sahin M. Photocatalytic hydrogen production by direct sunlight: a laboratory experiment. J Chem Edu 2003;80 (11): 1314–5.

[3] Li Y, Lu G, Li S. Photocatalytic hydrogen generation and decomposition of oxalic acid over platinized TiO₂. Appl Catal A 2001;214:179–85.

[4] Takata T, Tanaka A, Hara M, Kondo JN, Domen K. Recent progress of photocatalysts for overall water splitting. Catal Today 1998;44:17–26.

[5] Nguyen TV, Kim KJ, Yang OB. Photocatalytic water decomposition for hydrogen production over silico-tungstic acid–silica photocatalyst. J Photochem Photobiol A 2005; 173:56 –63.

[6] Buhler N, Meier K, Reber JF. Photochemical hydrogen production with cadmium sulfide suspensions. J Phys Chem 1984;88:3261–8.

[7] Sant PA, Kamat PV. Interparticle electron transfer between size-quantized CdS and TiO₂ semiconductor nanoclusters. Phys Chem Chem Phys 2002;4:198–203.

[8] Kakuta N, Park KH, Finlayson MF, Ueno A, Bard AJ, Campion A, Fox MA, Webber SE, White JM. Photoassisted Hydrogen production using visible light and coprecipitated ZnS-CdS without a noble metal. J Phys Chem 1985;89: 732–4.

[9] Kida T, Guan G, Yoshida A. LaMnO₃/CdS nanocomposite: a new photocatalyst for hydrogen production from water under visible light irradiation. Chem Phys Lett 2003;371:563–7.

[10] Guan G, Kida T, Kusakabe K, Kimura K, Fang X, Ma T, Abe E, Yoshida A. Photocatalytic H₂ evolution under visible light irradiation on CdS/ETS-4 composite. Chem Phys Lett 2004;385:319–22.

[11] Supriya VT, Subrahmanyam M. Enhanced photocatalytic H₂ production over ZnS-CdS supported on super basic oxides. Int J Hydrogen Energy 1998;23:741–4.

[12] Subrahmanyam M, Supriya VT, Ram Reddy P. Photocatalytic H₂ production with CdS-based catalysts from a sulphide/ sulphite substrate: an effort to develop MgO-supported catalyst. Int J Hydrogen Energy 1996;21:99–106.

[13] Pal B, Torimoto T, Iwasaki K, Shibayama T, Takahashi H, Ohtani B. Size and structure-dependent photocatalytic activity of jingle-bell-shaped silica-coated cadmium sulfide nanoparticles for methanol dehydrogenation. J Phys Chem B 2004;108:18670–4.

[14] Warrier M, Lo MKF, Monbouquette H, Garcia-Garibay MA. Photocatalytic reduction of aromatic azides to amines using CdS and CdSe nanoparticles. Photochem Photobiol Sci 2004;3:859–63.

[15] Chen YT, Ding JB, Guo Y, Kong LB, Li HL. A facile route to preparation of CdS nanorods. Mater Chem Phys 2002;77: 734–7.

[16] Wang W, Liu Z, Zheng C, Xu C, Liu Y, Wang G. Synthesis of CdS nanoparticles by a novel and simple one-step, solid-state reaction in the presence of a nonionic surfactant. Mater Lett 2002;4238:1–6.

[17] Parvathy NN, Pajonk GM, Venkateswara Rao A. Synthesis of various size CdS nanocystals in porous silica matrix and their spectral and physical properties. Nanostrict Mater 1997;8: 929–43.

[18] Liem N, Richard K, Weon B, Rajesh KM. Glutathione as a matrix for CdS nanocrystallites. Chemosphere 1999;38: 155–73.

[19] Wellmann H, Rathousky J, Wark M, Zukal A, Schulz-Ekloff G. Formation of CdS nanoparticles within functionalized siliceous MCM-41. Microporous Mesoporous Mater 2001;44–45:419–25.

[20] Pattabi M, Uchil J. Synthesis of Cadmium Sulphide nanoparticles. Sol Energy Mater Sol Cells 2000;63:309–14.

[21] Peng T, Yang H, Dai K, Pu X, Hirao K. Fabrication and characterization of CdS nanotube arrays in porous anodic aluminum oxide templates. Chem Phys Lett 2003;379:432–6.

[22] Tandon SP, Gupta JP. Measurement of forbidden energy gap of semiconductors by diffuse reflectance technique. Phys Status Solidi 1970;38:363–7.

[23] Sakata T, Kawai T, Hashimoto K. Photochemical diode model of platinum/titanium dioxide particle and its photocatalytic activity. Chem Phys Lett 1982;88:50–4.

[24] Ranjit KT, Varadarajan TK, Viswanathan B. Photocatalytic reduction of nitrogen to ammonia over noble metal-loaded TiO_2. J Photochem Photobiol A 1996;96:181–5.